



## Temperature effects on growth and biochemical composition of *Chlorella vulgaris* under heterotrophic cultivation

Jinjing Yin<sup>\*</sup> , Wendie Levasseur<sup>✉</sup> , Victor Pozzobon<sup>✉</sup> 

Université Paris-Saclay, CentraleSupélec, Laboratoire de Génie des Procédés et Matériaux, Centre Européen de Biotechnologie et de Bioéconomie (CEBB), 3 rue des Rouges Terres, 51110, Pomacle, France

### ARTICLE INFO

**Keywords:**  
Microalgae  
Temperature  
Growth  
Biochemical composition  
Lipid profile

### ABSTRACT

Temperature, despite being one of the key environmental factors influencing the physiology and metabolism of microalgae, is often overlooked. Most studies investigating temperature effects in microalgae mainly focus on phototrophic cultivation where the combined effects of light and temperature make it difficult to attribute observed physiological and biochemical changes effects to temperature alone. In contrast, heterotrophic cultivation, which relies on organic carbon sources and grow without light, allows a more direct assessment of temperature effects. However, studies investigating the influence of temperature on microalgae under heterotrophic conditions are extremely limited. However, investigations on how temperature influences microalgae under heterotrophic conditions are limited. In this study, the growth, biochemical composition, and fatty acid profile of *Chlorella vulgaris* across a broad temperature range (4–35 °C) under heterotrophic conditions were first investigated. The results showed that growth was optimal at 25–30 °C, while it was strongly inhibited at 35 °C. Temperature had significant effects on biomass composition: lipids were enhanced at high temperatures (30 °C, 35.49 ± 3.58%), pigments accumulated at low temperature (4 °C, 16.33 ± 2.93 mg/g DW), while proteins and carbohydrates peaked under moderate temperatures (15 °C, 18.71 ± 1.51%, 49.33 ± 1.74%, respectively). Fatty acid composition was temperature dependent, with monounsaturated fatty acids decreasing at higher temperatures, and polyunsaturated fatty acids showing opposing trends (especially C18:2n6c and C18:3n3), and saturated fatty acids remaining relatively stable. These findings highlight the physiological plasticity of *Chlorella vulgaris* under heterotrophic conditions and provide new insights into the thermal regulation of microalgal metabolism, with valuable implications for industrial biotechnology.

### 1. Introduction

Microalgae, also known as phytoplankton in ecological studies, are unicellular or colony-forming photosynthetic organisms typically 1–50 µm in size, inhabiting not only diverse aquatic environments from freshwater to oceans but also terrestrial environments such as soils. As primary producers in the marine food chain, they efficiently perform photosynthesis, converting CO<sub>2</sub> and water into oxygen and nutrient-dense biomass. This ability is supported by their broad tolerance to a wide range of temperatures, salinities, pH levels, CO<sub>2</sub> levels, and light conditions (Serra-Maia et al., 2016; Gao et al., 2023). With over 100,000 identified species, microalgae are classified based on morphology, pigments, life cycles and genomic information, commonly into *Chlorophyta*, *Bacillariophyta*, *Cyanobacteria*, *Dinoflagellata*, *Euglenophyta*, *Haptophyta*, *Cryptophyta* and *Glaucophyta* (Guiry and Guiry, 2025).

Nowadays, microalgae are considered a potential sustainable resource of great interest due to their fast growth rate, high photosynthetic efficiency and their ability to produce a wide range of valuable bioactive compounds such as antioxidants, pigments, protein and lipids (Levasseur et al., 2020). Additionally, they can grow using wastewater and industrial waste gases like CO<sub>2</sub> and NO<sub>x</sub>, thereby contributing to pollutant reduction (Zhao et al., 2024). Given their biotechnological and ecological relevance, microalgae are expected to play a key role in addressing global challenges, for example by contributing to biodiversity conservation through carbon sequestration and ecosystem support, and by promoting the transition toward a circular bioeconomy through sustainable production of bio-based compounds. Given their ecological and commercial relevance, microalgae are expected to play a key role in addressing global challenges, for example by contributing to biodiversity conservation through carbon sequestration and ecosystem support,

<sup>\*</sup> Corresponding author

E-mail address: [jinjing.yin@centralesupelec.fr](mailto:jinjing.yin@centralesupelec.fr) (J. Yin).

<https://doi.org/10.1016/j.plaphy.2026.111431>

Received 2 February 2026; Received in revised form 6 May 2026; Accepted 26 May 2026

Available online 27 May 2026

0981-9428/© 2026 The Authors. Published by Elsevier Masson SAS. This is an open access article under the CC BY-NC license (<http://creativecommons.org/licenses/by-nc/4.0/>).

and by promoting the transition toward a circular bioeconomy through sustainable production of bio-based compounds.

Among various microalgal species, *Chlorella vulgaris* has been extensively studied, particularly for the ability to accumulate valuable macromolecules such as lipids, proteins, and carbohydrates (Ru et al., 2020; Safi et al., 2014). Moreover, it can grow under different cultivation modes, including photoautotrophy, mixotrophy, and heterotrophy, making it a model organism for both basic research and industrial applications (Kim and Hur, 2013; Liang et al., 2009; Sajadian et al., 2018; Zhang et al., 2014). In addition, the long historic use of *C. vulgaris* as food and feed in Japan highlights its safety and supports its potential as a scalable and sustainable microalgal cultivation candidate.

However, the performance of *C. vulgaris* strongly depends on environmental conditions, among which temperature is one of the most important factors regulating photosynthesis, metabolism, enzyme activity, nutrient utilization, but it is often overlooked (Chokshi et al., 2015). Generally, microalgae can generally grow over a wide temperature range, with many species growing between 15 and 30 °C (González-Camejo et al., 2019), but efficient and stable biomass production is often achieved within a narrower window of 20–25 °C (da Silva Ferreira and Sant'Anna, 2017).

Still, when it comes to the investigation of temperature effects on microalgae culture, phototrophy and heterotrophy show large discrepancy, with only 10 % of the studies focusing on the latter. This imbalance is consistent with the broader underrepresentation of heterotrophy research in microalgae scientific community, where heterotrophic studies account for only 4–5% of the total scientific production according to our bibliometric analysis (Fig. S1). It can be explained by the fact that large-scale production of photosynthetic microalgae can only be envisioned outdoors, and outdoor production systems are directly affected by solar flux, with high daily and seasonal temperature variations (Béchet et al., 2010). These variations can affect both growth and biochemical composition. Industrially, heterotrophic cultivation is already used by major producers, particularly in Europe, as it enables controlled, high cell density microalgal production (Lu et al., 2024). Therefore, a deeper understanding of how temperature modulates heterotrophic microalgal physiology and metabolism was essential for optimizing productivity in large-scale cultivation systems.

From these phototrophy-focused researches, several trends have been identified, as temperature increases, microalgal growth typically increases until it reaches the optimal temperature. However, when the temperature exceeds or does not reach the optimal range for a species, microalgal growth will decrease or even be inhibited, ultimately leading to death (Ievina and Romagnoli, 2024; Ras et al., 2013). Besides, temperature also affects microalgal cell morphology, biochemical composition, and nutrient requirements. For example, the increasing temperature is often associated with reduced cell size (Barten et al., 2021; Peter and Sommer, 2013). Meanwhile, when temperature exceeds the optimal range, characteristic macronutrients shift was observed: protein content tends to increase due to the synthesis of stress-response proteins (Wang et al., 2023; Zhu et al., 1997), lipid accumulation generally declines (Gao et al., 2023; Xin et al., 2011), and carbohydrate and starch reserves are enhanced (Chokshi et al., 2015; Han et al., 2013).

Still, the applicability of those findings to heterotrophy remains questionable. Indeed, in phototrophy respiration (temperature-dependent) and photosynthesis (light and temperature-dependent) interplay at a profound metabolic level, which is not the case in heterotrophy. The need for investigations dedicated to the effect of temperature on microalgae heterotrophic growth is all the more urgent as this mode of production is more and more regarded as a promising alternative for large-scale biomass production (Barros et al., 2019; Shi et al., 2006). Additionally, the relevance of temperature is further highlighted by its role in structuring microbial communities in natural aquatic systems. In stratified lakes, Lepère et al. (2010) showed that picoeukaryotes communities segregate strongly along thermal

gradients: warm, illuminated surface layers are dominated by photosynthetic taxa, whereas colder and darker hypolimnia harbor mainly heterotrophic lineages. Notably, *Chlorophyta* were detected even below the euphotic zone, indicating that many taxa rely on facultative heterotrophy or mixotrophy to maintain activity in cold, low or no light heterotrophic depths. These depth-dependent shifts illustrate how temperature governs microbial metabolism and carbon-use strategies, providing an environmental perspective on why understanding temperature sensitivity is essential for assessing whether tight temperature control is needed in heterotrophic bioprocesses.

Overall, this study aims to investigate how temperatures ranging from 4 to 35 °C affect cell growth, biochemical composition, and fatty acids profile of *Chlorella vulgaris* under heterotrophic cultivation. Principal component analysis (PCA) and structural equation modeling (SEM) were selected further to explore the relationships among these responses. Therefore, this study can provide new insights into the thermal regulation of heterotrophic metabolism in microalgae and its implications for industrial biotechnology.

## 2. Materials and methods

### 2.1. Strain and culture medium

The strain used for this study was *Chlorella vulgaris* (CV 211-11b) obtained from SAG Culture Collection, Germany. Cells were cultivated in 2×B3N medium (Table S1) with 20 g/L glucose, at 30 °C under 100 rpm agitation in a dark incubator. The medium contained main nutrients: NaNO<sub>3</sub>, CaCl<sub>2</sub>·2H<sub>2</sub>O, MgSO<sub>4</sub>·7H<sub>2</sub>O, K<sub>2</sub>HPO<sub>4</sub>, KH<sub>2</sub>PO<sub>4</sub>, NaCl, EDTA, KOH, FeSO<sub>4</sub>·7H<sub>2</sub>O, H<sub>2</sub>SO<sub>4</sub>, H<sub>3</sub>BO<sub>3</sub>, ZnSO<sub>4</sub>·7H<sub>2</sub>O, MnCl<sub>2</sub>·4H<sub>2</sub>O, MoO<sub>3</sub>, CuSO<sub>4</sub>·5H<sub>2</sub>O, Co(NO<sub>3</sub>)<sub>2</sub>·6H<sub>2</sub>O, and they are based on B3N medium described by Andersen (2005). They were subcultured every 2 weeks and used as inoculum for further experiments.

### 2.2. Culture protocol

The cells were cultivated in 250 mL Erlenmeyer flasks (25 mL medium, 100 rpm, in dark) at six different temperatures: 4, 15, 20, 25, 30 and 35 °C. Before monitoring the culture at different test temperatures, cells were subcultured under each condition for more than three generations to make sure acclimation to the test temperature. At each test temperature, eight biological replicates were cultivated (n = 8), along with two flasks as blank controls (25 mL ultrapure water) to monitor evaporation. The eight replicate flasks were separately inoculated with 1% (v/v) inoculum from the same homogenized pre-acclimated subculture and then cultivated independently. Flasks were randomly positioned to minimize positional bias, and the temperature of each flask was individually monitored throughout the experiment. For each temperature, the experiment was repeated twice to guarantee reproducibility.

### 2.3. Growth monitoring and analysis

For all the cultures, growth curve and temperature were automatically measured online with the cell growth quantifier (CGQ, Aquila Biolabs, Baesweiler, Germany) and data recorded by the software DOTS 1.3.3. Before harvesting, a calibration curve was conducted using eight biological replicates, with each point measured five times and averaged, linking to absorbance and dry weight (6 points, range from 0.06 to 6.92 g/L, R<sup>2</sup> = 0.9963, Fig. S2). Evaporation rates were derived from blank flasks, and OD values were corrected by evaporation before converting to the biomass content.

Cell growth rate ( $\mu$ ) was calculated in the exponential phase using the following equation:

$$\mu(\text{d}^{-1}) = \frac{\ln(C_{t_2}) - \ln(C_{t_1})}{t_2 - t_1} \quad (1)$$

where  $C_{t1}$  and  $C_{t2}$  are the biomass content (g/L) at time  $t_1$  and  $t_2$  (days), corresponding to the beginning and ending of the exponential phase.

To generalize the effect of temperature on specific growth rates ( $\mu$ ,  $\text{day}^{-1}$ ), data were fitted with a non-linear thermal performance model. The Logan equation was selected as the model not only because it allowed for fitting the data adequately with a minimal number of parameters, but also because it captures the main phenomenology observed in this study: an activation of metabolism with increasing temperature, followed by inhibition when temperature becomes too high. The model was initially developed for arthropods, particularly insects (Logan et al., 1976), and later modified by Tomlinson and Phillips (2015). Although the model was initially developed for arthropods, particularly insects, these organisms, like microalgae, are unable to regulate their internal temperature and are strongly driven by external temperature. Model performance was evaluated using the coefficient of determination ( $R^2$ ), Mean Average Percent Error (MAPE) and Akaike's Information Criterion (AIC). The final fit showed good agreement with the data ( $R^2 = 0.9479$ , MAPE = 9.56%, AIC = -212.025). The equation is as follows:

$$\mu(T) = \mu_0 (e^{bT} - e^{(T-T_{\text{inf}})}) \quad (2)$$

Where  $\mu_0$  is the reference growth rate ( $\text{day}^{-1}$ ),  $b$  is the temperature dependence ( $^{\circ}\text{C}^{-1}$ ),  $T_{\text{inf}}$  is the inflection temperature ( $^{\circ}\text{C}$ ), and  $T$  is the temperature ( $^{\circ}\text{C}$ ).

## 2.4. Biochemical composition analysis

The cells were harvested at the end of the exponential growth phase by centrifugation at 11,000 rpm for 10 min at 4  $^{\circ}\text{C}$  (5804 R, Eppendorf, Germany), and washed twice with ultrapure water. Then they were freeze dried (Alpha 1-2 LDplus, Christ, Germany) for 24 h and stored at -20  $^{\circ}\text{C}$  in dark for further analysis.

### 2.4.1. Pigment profile

For the extraction of pigments, 2-4 mg samples were resuspended with ultrapure water, then centrifuged to remove the supernatant (11000 rpm, 4  $^{\circ}\text{C}$ , 10 min). After that, samples were homogenized in 5 mL methanol by MP Biomedicals FastPrep42 bead beater (6.5  $\text{m s}^{-1}$  in two cycles of 30 s with a 60 s pause). According to the suggestion of Porra (1990), the suspension was heated in water bath for 20 min at 60  $^{\circ}\text{C}$ . After cooling down, the extract was filtered (0.22  $\mu\text{m}$ ) and absorbance spectrum was recorded from 340 to 800 nm with a precision of 0.2 nm (Shimadzu UV-1800). Finally, the concentrations of chlorophyll *a*, chlorophyll *b*, and total carotenoids ( $\mu\text{g pigment/mL supernatant}$ ) were calculated based on following equations (Lichtenthaler and Buschmann, 2001):

$$\text{Chl}_a = 16.72 A_{665.2 \text{ nm}} - 9.16 A_{652.4 \text{ nm}} \quad (3)$$

$$\text{Chl}_b = 34.09 A_{652.4 \text{ nm}} - 15.28 A_{665.2 \text{ nm}} \quad (4)$$

$$\text{Car}_{c+x} = (1000 A_{470 \text{ nm}} - 1.63 \text{Chl}_a - 104.96 \text{Chl}_b) / 221 \quad (5)$$

where  $A_{665.2 \text{ nm}}$ ,  $A_{652.4 \text{ nm}}$ ,  $A_{470 \text{ nm}}$  are the measured absorbances of the pigment extracts at specific wavelength.

### 2.4.2. Protein content determination

The protein content was quantified by TOC-L CSH analyzer (Shimadzu). Briefly, 2 mg sample (record as *m*) was resuspended into 20 mL ultrapure water and then for the analysis of total nitrogen content (TN; mg/L). Then the protein content was calculated using a protein-to-nitrogen conversion factor of 4.57, as established by Lourenço et al. (2004) for *Chlorella*, based on following equation:

$$\text{Protein (\%)} = \frac{4.57 \times \text{TN} \times 20}{m} \times 100 \quad (6)$$

### 2.4.3. Lipid content determination

The total lipid content was conducted by the procedure described by Bligh and Dyer (1959) with slight modifications. 20 mg samples were rehydrated in 1.6 mL ultrapure water, then 4 mL methanol, 2 mL chloroform, and 1 mL sand were added. After vortex, cells were disrupted in MP Biomedicals FastPrep42 bead beater (6.5  $\text{m s}^{-1}$  in two cycles of 30 s with a 60 s pause). Then they were mixed with 2 mL chloroform and 2 mL ultrapure and centrifuged (11000 rpm, 4  $^{\circ}\text{C}$ , 1 min) for phase separation. The chloroform phase containing the lipids were collected for evaporation, and residues were weighted for the lipid content calculation. The lipid content of microalgae was calculated through the division of the residue weight by the freeze-dried cell weight.

### 2.4.4. Ash quantification

The ash content was measured according to ISO 5984:2002 (International ceramic Organization for Standardization, 2002). Briefly, 20 mg lyophilized biomass was added in to constant weight crucibles (550  $^{\circ}\text{C}$ , 1 h), then all the crucibles were transferred to the muffle oven and heated at 550  $^{\circ}\text{C}$  for 3 h. After heating, the crucibles were placed in a desiccator, cooled to room temperature and then weighed for the calculation of ashes.

### 2.4.5. Carbohydrate content determination

The carbohydrate content was calculated by subtracting the measured percentages of lipids, proteins, pigments, and ash from the total cellular composition (100%).

## 2.5. Fatty acids methyl ester (FAME) profile determination

In-situ transesterification method was utilized following the instruction from the National Renewable Energy Laboratory (NREL) (Van Wychen et al., 2016). The extracts of FAMES were analyzed by GC-2010 Plus coupled to a GCMS-TQ8040 triple quadrupole mass spectrometer (Shimadzu) equipped with a HP-88 capillary column (100  $\text{m} \times 0.25 \text{ mm} \times 0.20 \mu\text{m}$ , Agilent). The helium (99.99% purity) was used as carrier gas with a linear velocity at a flow rate of 2 mL/min. Splitless mode was used for sample injection (1 mL, 240  $^{\circ}\text{C}$ ). The total run time was 34.5 min, and the running condition was as follows: the column temperature started at 50  $^{\circ}\text{C}$  for 1 min, then increased to 180  $^{\circ}\text{C}$  at the rate of 20  $^{\circ}\text{C}/\text{min}$  and held at 180  $^{\circ}\text{C}$  for 5 min. After which the temperature increased continuously to 200, 210, 220 and 230  $^{\circ}\text{C}$  at a rate of 10  $^{\circ}\text{C}$ , and maintained for 5, 5, 1 and 6 min, respectively. Detection was operated by the triple quadrupole in Electron Ionisation (EI) mode and the energy was 70 eV. The injector temperature was set at 210  $^{\circ}\text{C}$  and the MS source was at 200  $^{\circ}\text{C}$ . Multiple Reaction Mode (MRM) was used for the acquisition and the compounds were identified by comparison the retention time with standards. C13:0 was used as an internal calibration and FAME standard was the Supelco 37 component FAME mix (CRM47885, Sigma-Aldrich).

## 2.6. Data processing

Data was first analyzed by one-way analysis of variance (ANOVA). Then if  $p < 0.05$ , Tukey's honestly significant difference (HSD) test was applied to identify the origin of the difference. All the results were presented as the average of replicate ( $n = 8$ ), while the error bars account for the standard deviation. Multivariate statistical analysis including principal component analysis (PCA) was performed by MetaboAnalyst 6.0. Before multivariate analysis, the data were subjected to Pareto scaling. To statistically assess differences among temperature groups, permutational multivariate analysis of variance (PERMANOVA) was also conducted based on Bray-Curtis dissimilarities with 999 permutations.

In addition to conventional statistical technique, Structural Equation

Modeling was used to infer the construction of an action model for temperature. Three latent variables were considered: membrane fluidity (often reported/alleged as modulated by temperature in phototrophy studies (Chen et al., 2008; Nalley et al., 2018; Sonmez et al., 2016)), metabolic activity (considered as concept encompassing the intensity of enzymatic activity and growth), and energy storage (a strategy commonly deployed by microalgae). Membrane fluidity was evaluated through PUFA and PUFA fractions as well as the ratio of unsaturated fatty acids to saturated fatty acids, taken as the reference. Metabolic activity was derived from growth rate (reference), protein content (proxy of enzymatic content), and ash content (proxy of the dilution/concentration effect). Finally, storage was probed using lipids content (reference) and carbohydrate content. The network was iterated to only keep relevant association ( $p < 0.05$ ) and reached a satisfactory MAPE (Mean Average Percent Error) of 9.4 %. A visualization of the network before parameterization is available in the supplementary materials (Fig. S3).

### 3. Results and discussion

#### 3.1. Temperature effect on the growth of *Chlorella vulgaris*

A temperature-dependent trend was observed (Fig. 1A): at 20 °C, 25 °C and 30 °C, cells exhibited a rapid biomass accumulation with short lag phases of approximately 2 days. At 15 °C, growth was slower with a lag phase of 3 days. In contrast, growth at 4 °C was markedly delayed, with an extended lag phase of 20 days, despite consecutive runs at 4 °C to ensure cold acclimation. Notably, at 35 °C, no obvious growth was observed throughout the cultivation period (over two weeks), indicating that this temperature exceeds the upper thermal tolerance of *C. vulgaris* under heterotrophic conditions. Specific growth rates ( $\mu$ , Fig. 1B) increased with temperature, ranging from  $0.32 \pm 0.01 \text{ day}^{-1}$  at 4 °C to  $1.14 \pm 0.08 \text{ day}^{-1}$  at 30 °C. Statistical analysis confirmed that the growth rate at 15 °C ( $0.44 \pm 0.03 \text{ day}^{-1}$ ) was significantly lower than at 20 °C, 25 °C and 30 °C but higher than at 4 °C ( $p = 0.002$ ). In addition, the growth rate at 20 °C ( $0.63 \pm 0.05 \text{ day}^{-1}$ ) was significantly lower than at 25 °C and 30 °C ( $p < 0.001$ ), highlighting the progressive increase in cell growth with increasing temperature. However, there is no significant difference observed between 25 °C and 30 °C ( $p > 0.05$ ), suggesting both temperatures are within the optimal growth range, as also reported by Yu et al. (2014).

The observed growth differences under different temperatures reflect the strong temperature sensitivity of cellular metabolism in *C. vulgaris*. Although cells were able to grow between 4 °C and 30 °C, growth was significantly slower at lower temperatures, especially at 4 °C, which is associated with reduced enzymatic activity that led to delayed nutrient uptake and cell cycle progression (Converti et al., 2009; Renaud et al., 2002). At low temperatures, microalgal cells may activate cold stress responses such as the induction of cold-shock proteins (CSPs) and membrane lipid remodeling to maintain membrane fluidity and ensure

metabolic function (Kania et al., 2023). For example, in psychrophilic microalgae such as *Xanthonema hormidioides*, CSP expression is significantly upregulated, acting as RNA chaperones to stabilize transcription and translation under cold conditions (Gao et al., 2023). However, these mechanisms do not fully compensate for the overall metabolic slowdown at lower temperatures. In contrast, optimal growth was observed between 25 and 30 °C, where enzymatic and metabolic processes operate more efficiently. At 20 °C, growth was moderate, reflecting suboptimal enzymatic activity and metabolic rates that were sufficient to sustain growth but not to achieve the maximum performance observed at 25 and 30 °C. It is worth noting that complete growth inhibition was observed at 35 °C in our study, suggesting thermal stress beyond the physiological threshold for *C. vulgaris* 211-11b. To verify that this was growth inhibition rather than cell death, cells were transferred back to 30 °C, where they grew again (Fig. S4). High temperature has been reported to induce oxidative stress in *Auxenochlorella protothecoides*, leading to the accumulation of reactive oxygen and nitrogen species, membrane disruption, and protein denaturation (Xing et al., 2022). Despite the activation of protective mechanisms, these changes can result in irreversible cellular damage. Although other strains of *C. vulgaris* have been reported to grow at 35 °C under photoautotrophic conditions in previous study, this highlights that cultivation mode, as well as strain-specific differences, can influence thermal tolerance (Josephine et al., 2022).

Moreover, the relationship between temperature and growth rates observed in this study matched the thermal performance curve described by the Logan model (Logan et al., 1976; Tomlinson and Phillips, 2015), with a reference growth rate  $\mu_0$  of  $0.2464 \pm 0.0054 \text{ day}^{-1}$ , a temperature dependence  $b$  of  $0.05362 \pm 0.0006 \text{ } ^\circ\text{C}^{-1}$ , and an inflection temperature estimated at  $31.0 \pm 0.1 \text{ } ^\circ\text{C}$ . The narrow confidence intervals obtained for the fitted parameters confirmed the robustness of the model, indicating that the growth response of *C. vulgaris* to temperature follows a typical asymmetric pattern, with rapid acceleration at sub-optimal temperatures and a sharp decline beyond the optimum.

#### 3.2. Temperature effect on biochemical composition

To further evaluate the effect of temperature on cellular composition, the major biochemical components of *C. vulgaris* (lipids, protein, carbohydrates, pigments and ashes) were analyzed (Fig. 2 and Table S2). The results are presented and discussed for each component in the following sections.

##### 3.2.1. Lipid content

Lipid content exhibited a non-linear response to temperature (Fig. 2A). The highest lipid content was observed at 30 °C ( $35.49 \pm 3.58\%$ ), followed closely by 25 °C ( $35.03 \pm 2.78\%$ ). Notably, a high lipid content was also found at 4 °C ( $32.71 \pm 1.77\%$ ), with no significant difference with 25 °C and 30 °C ( $p = 0.389$  and  $p = 0.218$ ). In contrast,

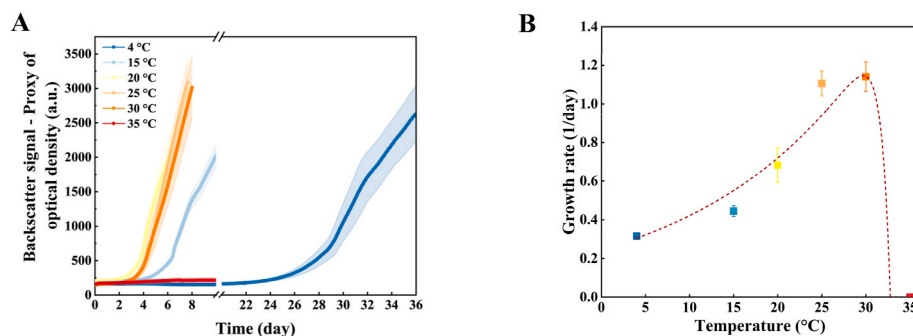


Fig. 1. (A) Growth curves and (B) Growth rate of *Chlorella vulgaris* cultivated at 4 °C, 15 °C, 20 °C, 25 °C, 30 °C and 35 °C. Data represents means  $\pm$  SD from eight biological replicates ( $n = 8$ ).

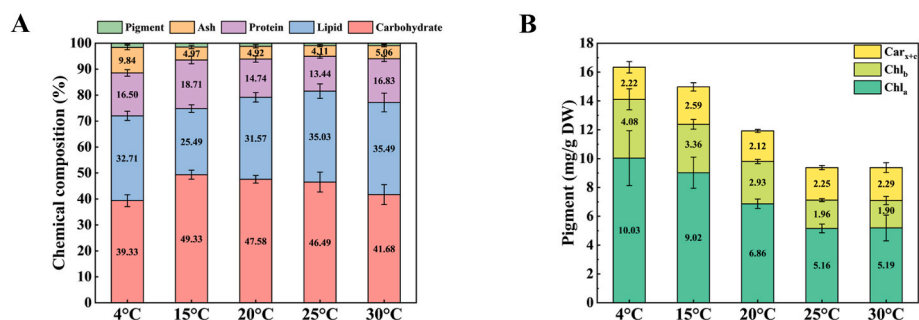


Fig. 2. (A) Chemical composition and (B) Pigment profile of *Chlorella vulgaris* cultivated under different temperatures (4 °C, 15 °C, 20 °C, 25 °C and 30 °C). Data represents means  $\pm$  SD from eight biological replicates ( $n = 8$ ).

lipid accumulation was significantly lower at 15 °C ( $25.49 \pm 1.45\%$ ,  $p < 0.001$ ). Cells cultivated at 20 °C showed middle lipid levels ( $29.46 \pm 2.87\%$ ), which differed significantly only from 30 °C ( $p = 0.034$ ).

Overall, lipid accumulation in *C. vulgaris* under heterotrophic conditions was strongly suppressed at 15 °C, whereas comparatively high levels were found at both 25 °C and 30 °C and even under cold stress at 4 °C, indicating that lipid accumulation in this strain under heterotrophy promoted at higher growth temperatures (25 °C and 30 °C) but can also be stimulated under cold stress (4 °C). A similar cold-associated increase has been described in some psychrotolerant green algae such as *Coccomyxa subellipsoidea* C-169, although in *C. vulgaris* the lipid content at 4 °C was comparable to that at 25–30 °C rather than being markedly higher (Kania et al., 2023). Meanwhile, temperature-stressed lipid responses have also been reported under heterotrophic conditions. In *Auxenochlorella protothecoides* UTEX 2341, both cold stress (10 °C) and heat stress (32 °C) promoted lipid accumulation compared with the control at 28 °C (Xing et al., 2018).

In fact, a comprehensive review of the literature reveals that most studies investigating the effect of temperature on lipid accumulation in microalgae have focused on the range between 20 °C and 30 °C (in both heterotrophy and phototrophy), with a few extending to higher temperatures such as 35 °C or even 40 °C. In contrast, research on temperatures below 20 °C was limited. Given the limited evidence in heterotrophy, phototrophic data were used to compare. As reported by Zhao et al. (2024), there was no difference in lipid content of *Cyclotella cryptica* when cultured at 25 and 29 °C, which was consistent with our results. However, when the temperature decreased to 17 °C, a significant increase in lipid content was found, suggesting that temperature effects on lipid biosynthesis were species-specific and highly dependent on other factors such as light.

Compared to 15 °C, the increased lipid content observed at 25 °C and 30 °C is consistent with the widely reported temperature-induced lipid accumulation in microalgae under heterotrophic or mixotrophic cultivation. A possible explanation is that high temperatures may enhance carbon metabolism, particularly glycolytic and the tricarboxylic acid (TCA) cycle, leading to an increased generation of acetyl-CoA and NADPH, which are essential for lipid biosynthesis. Due to the lack of transcriptomic data under heterotrophy, insights from phototrophic studies provide useful references. For example, transcriptomic analyses of *Tetraselmis* sp. Exposed to higher temperature under phototrophic conditions further support this hypothesis, indicating upregulation of mitochondrial genes involved in oxidative phosphorylation and phospholipid biosynthesis, which suggested an increased demand for energy and carbon flux redistribution under thermal stress (Shin et al., 2016). Moreover, *Chlorella vulgaris* under combined heat or nitrogen stress has been shown to downregulate protein synthesis and nitrogen assimilation, redirecting carbon toward storage lipids such as TAGs.

The relatively high lipid content was also observed at 4 °C, suggesting that cold stress can also trigger lipid accumulation, though the mechanism differs from high temperature. One possible explanation is that under rapid growth conditions, the relative lipid content may

decrease because other biomass components, such as proteins and carbohydrates, may accumulate at a faster rate. On the contrary, at low temperatures, the growth rate of *C. vulgaris* was significantly slowed, which may reduce this effect and contribute to a higher relative lipid content. Consequently, cell components such as lipids can be accumulated. As reported by Zhang et al. (2016), low temperatures limit cell growth and cell proliferation, thus reducing biomass dilution while maintaining or only moderately suppressing lipid biosynthesis, resulting in higher lipid content per algal biomass. In addition to the physical effect, the increase in lipid accumulation at low temperatures can be partially explained by stress-induced metabolic reallocation. Although Shin et al. (2016) focused on the fatty acids profiles change of *Tetraselmis* sp. Under cold conditions, their findings also implied that total lipid accumulation may also be promoted at low temperatures as an adaptive response to maintain membrane fluidity, particularly in chloroplast thylakoid membranes.

### 3.2.2. Protein content

The protein content varied with temperature change ( $p < 0.05$ ), the highest protein accumulation was observed at 15 °C ( $18.71 \pm 1.51\%$ ) (Fig. 2A), followed by 4 °C ( $16.50 \pm 1.26\%$ ) and 30 °C ( $16.83 \pm 1.02\%$ ) which are not significantly different ( $p > 0.05$ ). However, the protein content significantly dropped at 20 °C ( $14.71 \pm 1.23\%$ ) and 25 °C ( $13.44 \pm 0.73\%$ ), with no significant difference between these two temperatures ( $p = 0.192$ ). This pattern is consistent with the finding reported by Xie et al. (2023), who showed that *Euglena gracilis* reached the higher protein content at 30 °C. A similar pattern of temperature-dependent protein variation was also observed in *Isochrysis galbana* TK1, where the highest protein content was found at 15 °C during the exponential growth phase (Zhu et al., 1997). The highest protein content observed at 15 °C in *C. vulgaris* may also be related to a combination of moderate growth rates and efficient nutrient assimilation, which potentially enables the accumulation of structural and functional proteins. These findings are supported by Zhou et al. (2025), who demonstrated that higher protein accumulation was observed in *Thalassiosira weissflogii* at moderate temperatures and decreased under both cold and heat stress, likely due to impaired nitrogen assimilation and metabolic reallocation toward carbon-rich storage compounds under stress conditions.

In contrast, the decline in protein content at 20 °C and 25 °C suggests a temperature-sensitive reallocation of cell metabolism, possibly from nitrogen-rich macromolecules toward carbon-rich compounds, primarily toward carbohydrates and then lipids. Under this condition, cells may prioritize energy storage instead of protein synthesis. Interestingly, protein content at 30 °C rebounded to a level at 4 °C, which is supported by previous study (Renaud et al., 2002). It can be explained by stress-induced synthesis of protective proteins and interference with enzyme regulators at increasing temperature. Meanwhile, stable protein levels at 4 °C could be attributed to reduced protein turnover and slower biomass accumulation, resulting in less dilution of intracellular proteins. In addition, the induction of CSPs may also contribute to maintaining

protein stability under cold conditions.

These results implied that protein metabolism in *C. vulgaris* is non-linearly affected by temperature, with both cold and heat stress leading to protein maintenance or stress-induced compensation, while intermediate high temperature (20 °C and 25 °C) results in a metabolic shift away from nitrogen-based biomass components.

### 3.2.3. Carbohydrate content

As shown in Fig. 2A, carbohydrate content in *C. vulgaris* showed temperature sensitivity, with the highest value at 15 °C ( $49.33 \pm 1.74\%$ ), followed by 20 °C ( $47.58 \pm 1.47\%$ ), and 25 °C ( $46.49 \pm 3.81\%$ ). All three were significantly higher than at 4 °C ( $39.33 \pm 2.29\%$ ) and 30 °C ( $41.68 \pm 3.83\%$ ) ( $p < 0.05$ ).

This difference suggests that the temperature-dependent variation in carbohydrate accumulation is species-specific and highly influenced by the cultivation mode. Under photoautotrophic conditions, carbohydrate accumulation is closely linked to photosynthetic carbon fixation and photosynthesis was gradually damaged by increasing temperature. Thus, the small amount of NADPH generated by reduced photosynthesis would be used to store energy in the form of starch, explaining the carbohydrate accumulation (Shin et al., 2016). In contrast, under heterotrophic mode, where carbon is supplied externally and metabolism is not from light-driven photosynthesis, temperature may affect carbohydrate accumulation through different metabolic pathways. Therefore, the temperature-dependent variation in carbohydrate content is likely not universal but depends strongly on both species and trophic mode.

The highest carbohydrate content at 15 °C, 20 °C and 25 °C suggests that moderate temperature promotes polysaccharide accumulation through a balanced metabolic state, which is consistent with a significant decrease in protein content at 20 °C and 25 °C, indicating that reduced protein synthesis may have redirected carbon flux from proteins toward carbohydrate storage. Moreover, low temperatures may limit glycolytic flux, leading to reduced sugars into fatty acids, and thus favor carbohydrate retention. The moderate decrease in carbohydrate content at 30 °C, despite remaining relatively high, may reflect enhanced carbon flux into lipid biosynthesis under higher temperatures. This is consistent with the inverse trend observed in lipid content (see Section 3.2.1) and supports the concept of a classic carbon partitioning shift from polysaccharides to energy-dense neutral lipids under thermal or nutrient stress (Converti et al., 2009). In addition, this observation is consistent with previous findings in *C. vulgaris*, where maximum starch accumulation occurred around 20–24 °C, but sharply declined at higher temperatures due to increased activity of starch-degrading enzymes like  $\alpha$ -glucan phosphorylase, outweighing carbon fixation processes such as RuBisCO activity (Nakamura and Miyachi, 1982). By contrast, the lowest carbohydrate level at 4 °C could be attributed to slow metabolic activity, where neither synthesis nor storage occurs efficiently. Moreover, increased demand for membrane remodeling under cold stress may divert carbon intermediates into lipid or pigment biosynthetic pathways.

### 3.2.4. Pigment content and composition

The total pigment content of *C. vulgaris* showed a clear decreasing trend with increasing cultivation temperature (Fig. 2A). It reached the highest amount at 4 °C ( $1.63 \pm 0.29\%$ ) and declined sharply at higher temperatures, with values of  $1.49 \pm 0.16\%$  at 15 °C,  $1.19 \pm 0.06\%$  at 20 °C,  $0.94 \pm 0.05\%$  at 25 °C, and  $0.94 \pm 0.15\%$  at 30 °C. The 42.33% reduction from 4 °C to 25 °C suggests a strong negative effect of temperature on total pigment accumulation. This indicates that low temperatures promote pigment accumulation, whereas higher temperatures inhibit pigment biosynthesis or promote degradation. These results are consistent with previous studies showing that thermal stress can inhibit chlorophyll biosynthesis or damage pigment-protein complexes, particularly under heterotrophic or nutrient-limited conditions. For example, in marine microalgae such as *Nannochloropsis oculata* and *Isochrysis* sp., higher temperatures have been shown to impair

photosystem II reaction center assembly and reduce chlorophyll-binding capacity, leading to overall pigment decline (Renaud et al., 2002). These patterns highlight that pigment levels primarily reflect temperature-driven cellular homeostasis and stress responses rather than light-dependent metabolism in *C. vulgaris* under heterotrophy. Therefore, the observed thermal sensitivity of pigments provides insight into how *C. vulgaris* reallocates metabolic resources under thermal stress and how temperature shapes its biochemical composition even in the absence of photosynthesis.

Due to the relatively low abundance of pigment content compared to the other components (less than 1.7% of total dry weight), it is plotted separately as shown in Fig. 2B to clearly display the difference of pigment level. As shown in Fig. 2B, pigments mainly accumulated at 4 °C (Chl a:  $10.03 \pm 1.90$  mg/g; Chl b:  $4.08 \pm 0.73$  mg/g) and 15 °C (Chl a:  $9.02 \pm 1.08$  mg/g; Chl b:  $3.36 \pm 0.34$  mg/g), with significantly higher than at 25 °C (Chl a:  $5.16 \pm 0.30$  mg/g,  $p < 0.001$ ; Chl b:  $1.96 \pm 0.10$  mg/g,  $p < 0.001$ ) and 30 °C (Chl a:  $5.19 \pm 0.89$  mg/g,  $p < 0.001$ ; Chl b:  $1.90 \pm 0.29$  mg/g,  $p < 0.001$ ). Cells at 20 °C showed intermediate level (Chl a:  $6.86 \pm 0.33$  mg/g; Chl b:  $2.93 \pm 0.15$  mg/g), significantly lower than at 4 and 15 °C ( $p < 0.01$ ) but higher than at 25 and 30 °C ( $p < 0.05$ ). In contrast, carotenoid content remained stable among the tested temperatures, with only a minor difference between 4 °C and 30 °C ( $p = 0.021$ ).

Pigments were reported to respond to temperature shift (Barten et al., 2021; Shi et al., 2006; Xing et al., 2022; Yu et al., 2014). However, at present, there are still limit studies that report the temperature-dependent pigment responses under heterotrophic conditions. Available heterotrophic studies suggest that different pigments may respond differently to temperature. Xing et al. (2022) reported in *Auxenochlorella protothecoides* under heterotrophic conditions that chlorophyll content was more strongly reduced under cold stress (10 °C), whereas carotenoid metabolism showed a distinct response under heat stress (32 °C), indicating different pigment adaptation strategies under opposite temperature stresses. Similarly, Shi et al. (2006) showed in *Chlorella protothecoides* CS-41 that lutein increased gradually from  $4.25$  to  $4.59$  mg g<sup>-1</sup> as temperature increased from 24 to 35 °C, indicating that rising temperature promoted lutein accumulation at the cellular level. In the present study, chlorophyll content decreased from 4 °C to 30 °C, whereas carotenoids remained comparatively more stable, suggesting that chlorophyll was more sensitive to temperature variation than carotenoids under heterotrophic conditions.

Overall, pigment composition in *C. vulgaris* was strongly influenced by cultivation temperatures. Chlorophylls, especially chlorophyll a, dominate at low temperatures, which may reflect enhanced structural pigment retention or cold-induced stabilization of pigment-protein complexes. In contrast, carotenoid content remained relatively stable across the tested temperature range, which is expected given their primary role in photoprotection and heat dissipation, making them less responsive to thermal variation compared to other components. These findings highlight the functional plasticity of microalgal pigment systems in response to thermal variation, which may be crucial for environmental acclimation and enhancing resilience to stress. In case cells would have to rely on photosynthesis again, pigment plasticity would be particularly important. Similar trends under temperature stress have been described for photosynthetic microalgae, where pigments dynamically adjust to sustain metabolic balance. For example, Barten et al. (2022). Conducted that in *Picochlorum* sp., chlorophyll a and b levels declined under supra-optimal temperatures (from 30 °C to 42 °C), while carotenoid contents were comparatively stable, underscoring the differential sensitivity of pigments to thermal stress.

### 3.2.5. Ash content

Ash content, representing the inorganic fraction of cellular biomass, was also influenced by cultivation temperature (Fig. 2A). The highest ash content was observed at 4 °C ( $9.84 \pm 0.87\%$ ), which was significantly higher than at all other temperatures ( $p < 0.001$ ). Among the

other temperatures, no significant differences were found at 15 °C ( $4.97 \pm 0.59\%$ ), 20 °C ( $4.92 \pm 0.62\%$ ), and 30 °C ( $5.06 \pm 0.45\%$ ), while the lowest content was observed at 25 °C ( $4.11 \pm 0.42\%$ ), significantly lower than at 30 °C ( $p = 0.029$ ). This trend indicated that extremely low temperature conditions promote ash accumulation (inorganic residue), while higher temperatures drive to promote organic biomass accumulation, leading to a relative reduction in inorganic content. The observed increase in ash content at 4 °C may be attributed to slower cell division rates, which limited dilution effect: as biomass accumulates and cells divide, intracellular mineral ions are normally distributed to daughter cells, lowering their relative proportion. Additionally, cold stress may trigger ionic adjustments to maintain osmotic balance and membrane functionality, such as the upregulation of  $K^+$ ,  $Ca^{2+}$ , and  $Mg^{2+}$  transport and sequestration mechanisms, which could contribute to higher ash yield under low temperatures, although direct experimental evidence in microalgae remains limited.

In contrast, the ash content measured for *C. vulgaris* between 15 and 30 °C remained consistently around 5.0 % on dry weight biomass, which are agreed with previous studies. For example, Jabeen et al. (2020) reported an ash content of 5.3 wt % in *C. vulgaris*. Moreover, in the seasonal variations in light intensity and temperature (23.2 °C–28 °C), Metsoviti et al. (2019) reported that the ash content of *C. vulgaris* remained stable across treatments, showing no significant changes in response to environmental fluctuations such as temperature and irradiance.

### 3.2.6. Principal component analysis (PCA) based on biochemical composition

To further get a clearer view in a multi-dimensional space of the overall impact of temperature on the biochemical composition of *Chlorella vulgaris*, a principal component analysis (PCA) was conducted. The first two principal components, PC1 and PC2, accounted for 72.4% of the total variance, with PC1 explaining 38.6% and PC2 explaining 33.8% (Fig. 3).

Samples clustered differently according to cultivation temperature, indicating strong temperature-driven biochemical differentiation in *C.*

*vulgaris*. As shown in PCA biplot (Fig. 3), cultures at 4 °C, 15 °C, 20 °C, 25 °C and 30 °C were clearly separated into distinct clusters, reflecting strong temperature-dependent shifts in biochemical composition. Notably, samples at 25 °C and 30 °C were positioned on the positive side of PC1 and showed partial overlap, indicating similar metabolic profiles under higher temperatures. In contrast, samples at 4 °C and 15 °C formed distinct clusters on the negative side of PC1, highlighting characteristic metabolic states under cold conditions, while those at 20 °C formed a unique cluster, highlighting a transitional metabolic state between cold and heat treatment. PC2 further contributed to the separation of the low temperature groups, especially distinguishing 4 °C from 15 °C. Although samples at 4 °C and 15 °C were both positioned on the negative side of PC1, samples at 15 °C showed higher PC2 scores. These distinct clusters likely reflect different physiological states induced by temperature, while a more detailed explanation of the physiological mechanisms based on the corresponding arrow in biplot, which further illustrates how specific biochemical parameters contributed to the observed clustering. Cells cultivated at 15 °C and 20 °C were positively associated with carbohydrate content, whereas those grown at 4 °C correlated with protein, chlorophyll *a* and *b*. In contrast, cells grown at 25 °C and 30 °C were linked with total lipids, total fatty acids, and growth rate, suggesting enhanced lipid-related metabolism and rapid proliferation under high temperature conditions. These findings clearly demonstrate that temperature triggers coordinated shifts in biomass composition, which can be interpreted as a physiological reprogramming strategy. Low temperatures are conducive to stress adaptation and structural components, while high temperatures are beneficial for storage lipid biosynthesis and biomass productivity.

### 3.3. Temperature effect on fatty acids profile

As illustrated in Fig. 4 and Table 1, the fatty acids composition was significantly influenced by cultivation temperature. Total fatty acids mainly comprised saturated fatty acids (SFA), monounsaturated fatty acids (MUFA), and polyunsaturated fatty acids (PUFA), and their relative proportions were changed under different temperature conditions.

#### 3.3.1. Detailed fatty acid responses to temperature

Overall, across all the temperatures, the most abundant SFA and MUFA were palmitic acid (C16:0) and oleic acid (C18:1n9c), respectively, while the major PUFA were linoleic acid (C18:2n6c) and linolenic acid (C18:3n3). This fatty acid profile is consistent with previous studies and represents the typical composition observed in green microalgae under both heterotrophy and phototrophy (Kim and Hur, 2013; Riccardo et al., 2024; Xin et al., 2011; Xing et al., 2018).

Among SFA, C16:0 increased significantly from  $14.89 \pm 0.58\%$  at 4 °C to  $16.60 \pm 0.17\%$  at 15 °C ( $p < 0.001$ ). Then it decreased at higher temperatures, with significantly lower at 20 °C ( $15.04 \pm 0.21\%$ ), 25 °C ( $14.16 \pm 0.18\%$ ), and 30 °C ( $14.16 \pm 0.18\%$ ) compared to 15 °C ( $p < 0.001$ ), while no significant difference was found between 20 °C and 25 °C. A similar trend has been observed in *Microglena antarctica*, where C16:0 tends to accumulate under lower temperature due to enhanced *de novo* synthesis (Riccardo et al., 2024). In contrast, C18:0 showed a sharp and continuous increase with temperature, rising from  $0.77 \pm 0.04\%$  at 4 °C to  $4.24 \pm 0.16\%$  at 30 °C, suggesting that fatty acids tend to increase saturation under thermal stress. As a dominant MUFA, C18:1n9c constituted the largest fraction of the total fatty acids under all temperatures. It reached the highest level at 4 °C ( $57.25 \pm 1.60\%$ ), whereas a significant decrease was found at 15 °C ( $51.44 \pm 0.93\%$ ,  $p < 0.001$ ). With increasing temperature, C18:1n9c increased to  $54.62 \pm 1.11\%$  at 25 °C and  $55.40 \pm 1.18\%$  at 30 °C, both significantly higher than at 15 °C ( $p < 0.001$ ) but still lower than at 4 °C ( $p < 0.001$ ). The consistently high proportion of C18:1n9c across all temperatures suggests stable  $\Delta 9$ -desaturase activity, which catalyzes the conversion of C18:0 to C18:1n9c. Previous studies have reported elevated levels of oleic acid in *Auxenochlorella protothecoides* under heterotrophic conditions,

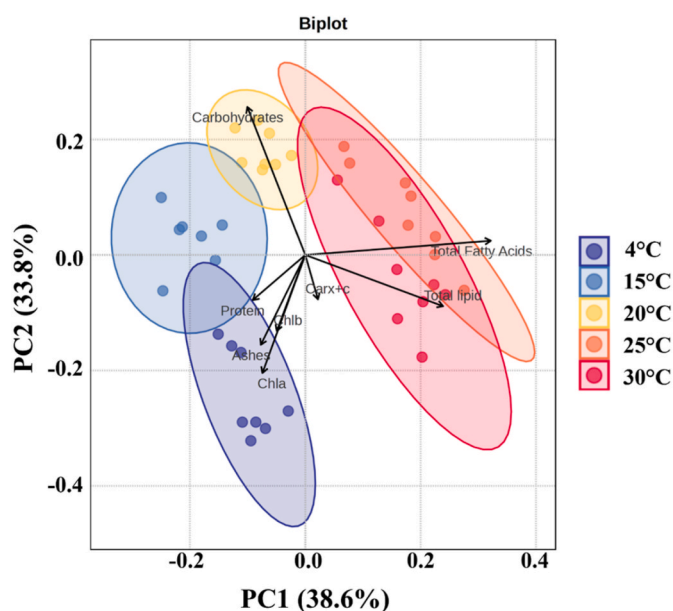
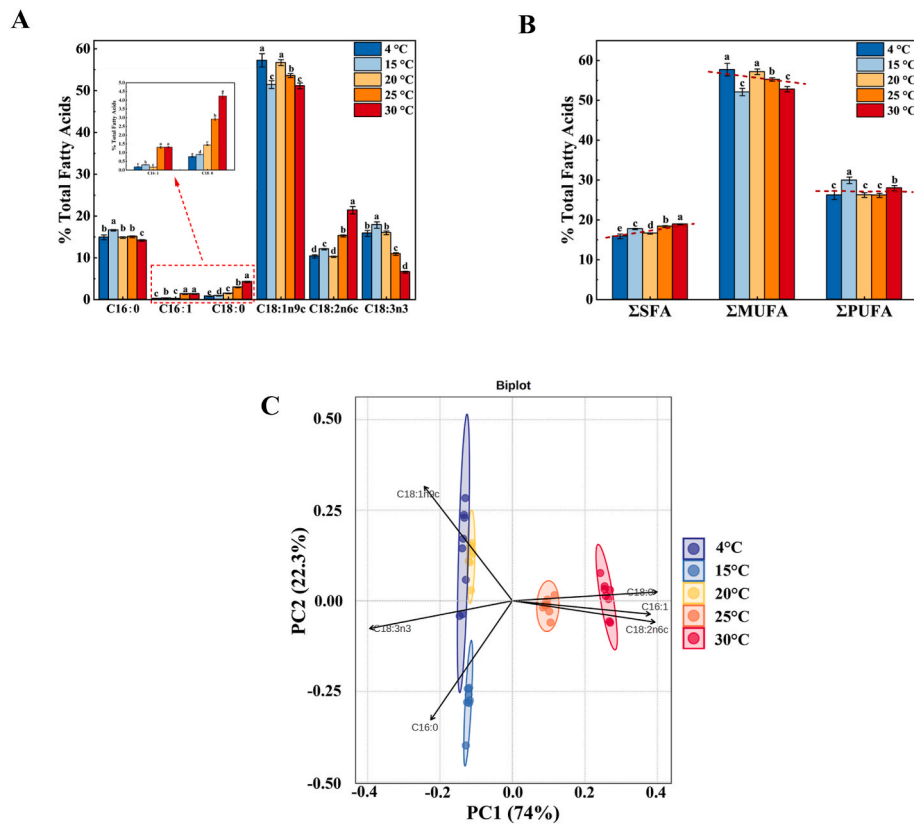


Fig. 3. Biplot of principal component analysis (PCA) based on chemical composition profile under different temperatures (4 °C, 15 °C, 20 °C, 25 °C and 30 °C). The x- and y-axes represent principal components 1 and 2, respectively, with the percentages of total variance explained by each axis shown in parentheses. PERMANOVA analysis confirmed that the metabolomes at different temperatures were significantly distinct ( $p < 0.001$ ).



**Fig. 4.** (A) Fatty acids composition and (B) fatty acids classes composition under different temperatures (4 °C, 15 °C, 20 °C, 25 °C and 30 °C); (C) Biplot of principal component analysis (PCA) based on fatty acids profile under different temperatures (4 °C, 15 °C, 20 °C, 25 °C and 30 °C). The x- and y-axes represent principal components 1 and 2, respectively, with the percentages of total variance explained by each axis shown in parentheses. PERMANOVA analysis confirmed that the metabolomes at different temperatures were significantly distinct ( $p < 0.001$ ). SFA – Saturated fatty acids; MUFA - Monounsaturated fatty acids; PUFA - Polyunsaturated fatty acids.

**Table 1**

Fatty acid composition (% of total fatty acids) of *Chlorella vulgaris* cultivated at 4 °C, 15 °C, 20 °C, 25 °C, and 30 °C (showing only fatty acids with relative abundance >1%, Means ± SD, n = 8). Different letters indicate significant differences among temperatures at  $p < 0.05$ .

Fatty acids	% total fatty acids				
	4 °C	15 °C	20 °C	25 °C	30 °C
C16:0	14.89 ± 0.58 <sup>b</sup>	16.60 ± 0.17 <sup>a</sup>	14.84 ± 0.18 <sup>b</sup>	15.04 ± 0.21 <sup>b</sup>	14.16 ± 0.18 <sup>c</sup>
C16:1	0.19 ± 0.01 <sup>c</sup>	0.30 ± 0.01 <sup>b</sup>	0.17 ± 0.01 <sup>c</sup>	1.31 ± 0.05 <sup>a</sup>	1.32 ± 0.04 <sup>a</sup>
C18:0	0.77 ± 0.04 <sup>c</sup>	0.89 ± 0.07 <sup>d</sup>	1.44 ± 0.03 <sup>c</sup>	2.92 ± 0.07 <sup>b</sup>	4.24 ± 0.16 <sup>a</sup>
C18:1n9c	57.25 ± 1.60 <sup>a</sup>	51.44 ± 0.93 <sup>c</sup>	56.71 ± 0.69 <sup>a</sup>	53.61 ± 0.47 <sup>b</sup>	51.16 ± 0.69 <sup>c</sup>
C18:2n6c	10.35 ± 0.39 <sup>d</sup>	12.06 ± 0.16 <sup>c</sup>	10.24 ± 0.16 <sup>d</sup>	15.25 ± 0.24 <sup>b</sup>	21.40 ± 0.87 <sup>a</sup>
C18:3n3	15.85 ± 0.72 <sup>b</sup>	17.86 ± 0.76 <sup>a</sup>	15.97 ± 0.44 <sup>b</sup>	10.92 ± 0.32 <sup>c</sup>	6.58 ± 0.23 <sup>d</sup>
ΣSFA	15.87 ± 0.58 <sup>e</sup>	17.72 ± 0.14 <sup>c</sup>	16.60 ± 0.16 <sup>d</sup>	18.34 ± 0.23 <sup>b</sup>	18.89 ± 0.13 <sup>a</sup>
ΣUSFA	83.64 ± 0.58 <sup>a</sup>	81.67 ± 0.15 <sup>c</sup>	83.09 ± 0.16 <sup>b</sup>	81.09 ± 0.22 <sup>d</sup>	80.46 ± 0.14 <sup>e</sup>
ΣMUFA	57.71 ± 1.58 <sup>a</sup>	52.07 ± 0.92 <sup>c</sup>	57.18 ± 0.69 <sup>a</sup>	55.24 ± 0.42 <sup>b</sup>	52.79 ± 0.68 <sup>c</sup>
ΣPUFA	26.20 ± 1.08 <sup>c</sup>	29.92 ± 0.81 <sup>a</sup>	26.23 ± 0.59 <sup>c</sup>	26.17 ± 0.53 <sup>c</sup>	27.98 ± 0.66 <sup>b</sup>
ΣUSFA/ΣSFA	5.35 ± 0.23 <sup>a</sup>	4.67 ± 0.04 <sup>c</sup>	5.10 ± 0.06 <sup>b</sup>	4.51 ± 0.07 <sup>d</sup>	4.37 ± 0.04 <sup>d</sup>

SFA – Saturated fatty acids; USFA – Unsaturated fatty acids; MUFA – Monounsaturated fatty acids; PUFA – Polyunsaturated fatty acids.

indicating that C18:1n9c serves as a key intermediate in triacylglycerol (TAG) biosynthesis (Xing et al., 2018).

In contrast, for PUFA, C18:2n6c increased from 10.35 ± 0.72% at 4 °C to 21.40 ± 0.72% at 30 °C, while α-C18:3n3 decreased from 17.86% at 15 °C to 6.58% at 30 °C, indicating temperature-sensitive regulation of desaturases such as Δ12 and Δ15. Similar temperature dependence of this desaturation cascade has been described in *Synechocystis* sp. PCC6803, where lower temperatures enhanced the activity of Δ12 and Δ15 desaturases, promoting the conversion of C18:1n9c to C18:2n6c and further to C18:3n3, while high temperatures inhibited these enzymatic pathways and consequently reduced PUFA levels (Chen et al., 2014). Additional support for a temperature-regulated

redistribution within the C18 pathway comes from studies in *Nannochloropsis oceanica*, where C18:2 decreased and C18:3 increased under low temperature conditions (Ferrer-Ledo et al., 2023). This pattern is consistent with observations in *Lobosphaera incisa*, in which the accumulation of C18:3 at low temperatures was attributed to a bottleneck in the elongation step converting C18:3 into long-chain PUFAs (Zorin et al., 2017). Therefore, these findings suggest that both desaturase-driven conversion and temperature-limited elongation contribute to the opposite temperature responses of C18:2 and C18:3 observed in *C. vulgaris*.

The distribution of fatty acid classes (Fig. 4B) further supported these observations: PUFA levels were significantly higher at 15 °C ( $p < 0.001$ ), whereas MUFA peaked at 4 °C, and SFA content remained relatively

stable but increased gradually with increasing temperatures. Regression analysis confirmed these tendencies, with SFAs displaying a weak positive correlation with temperature (+0.13% per °C,  $p = 0.11$ ), while MUFAs tended to decrease (-0.12% per °C,  $p = 0.53$ ) and PUFAs remained essentially unchanged level (-0.01% per °C,  $p = 0.93$ ). Although these slopes were not statistically significant, this trend still suggested a temperature-induced shift from unsaturated to saturated/monounsaturated fatty acids, which are believed to contribute to maintain membrane integrity and energy storage under different temperatures (Sakamoto and Murata, 2002).

### 3.3.2. Principal component analysis (PCA) based on fatty acids

To further characterize the influence of temperature on fatty acid profiles, principal component analysis (PCA) was conducted. The PCA biplot (Fig. 4C) based on fatty acid composition revealed distinct clustering of *Chlorella vulgaris* according to cultivation temperature. The five groups (4 °C, 15 °C, 20 °C, 25 °C, and 30 °C) were clearly separated along PC1 (74%) and PC2 (22.3%), which together explained 96.3% of the total variance, indicating that fatty acids composition were significantly different at tested temperature. Cells grown at 4 °C and 15 °C grouped on the negative PC1 axis, while those at 25 °C and 30 °C were located on the positive PC1 side, reflecting opposing trends in fatty acid profiles and indicating a clear temperature-driven separation in fatty acids composition. Cells grown at 20 °C also clustered on the negative PC1 side but were slightly shifted toward the center compared to 4 °C and 15 °C. The corresponding biplot arrow further illustrated how individual fatty acids contributed to the observed clustering.

Cells grown at 4 °C, 20 °C and 15 °C were closely associated with C18:3n3, C18:1n9, and C16:0, reflecting a PUFA enriched profile with contributions from short-chain saturated fatty acids. In contrast, cells cultured at 25 °C and 30 °C were strongly associated with C 16:1, C18:2n6, C18:0, and other long-chain saturated fatty acids (data not shown), suggesting a shift toward more saturated lipids, especially the long-chain saturated fatty acids. The PCA results highlighted a temperature-dependent remodeling of fatty acid composition in *Chlorella vulgaris*, as reported by Thompson (1996), where low temperatures contained more unsaturated fatty acid (especially PUFA), while higher temperatures promote MUFA and SFA production, supporting energy storage or thermally stable membranes.

### 3.4. Structural equation modeling (SEM) analysis of temperature-driven changes

Structural equation modeling (SEM) revealed a coordinated network

through which temperature regulates cellular metabolism and biochemical composition in heterotrophically grown *C. vulgaris* (Fig. 5). Increasing temperature exerted two primary effects: a reduction in membrane fluidity (-0.035,  $p < 0.001$ ) and a promotion of cell metabolism (0.035,  $p < 0.001$ ). These responses acted as upstream regulatory nodes that propagated thermal effects to downstream metabolic and compositional traits through both direct and indirect pathways.

The temperature-fluidity axis drove pronounced remodeling of the fatty acid profile. Reduced fluidity at increased temperatures strongly increased MUFA accumulation (5.062,  $p < 0.001$ ) while decreasing PUFA content (-1.864,  $p < 0.001$ ), a pattern consistent with the need to stabilize membrane viscosity under warmer conditions. These connected pathways indicate that temperature reshapes the fatty acid profile not by acting directly on individual lipid groups, but by modulating membrane physical properties, which then drive the redistribution between PUFA and MUFA.

Temperature also influenced cell composition through a second major route: metabolic activity, which subsequently exerted strong regulatory influence on biochemical components (including energy storage means). Metabolic activity positively affected proteins (4.037,  $p < 0.001$ ), while strongly suppressing ash content (-3.165,  $p < 0.001$ ). In addition, there is a significant positive indirect effect between metabolic activity and storage (0.197,  $p = 0.02$ ). And storage exerted additional direct effects on carbohydrates (-0.959,  $p < 0.001$ ), with lipid taken as reference. Notably, these direct storage effects coexist with indirect metabolic pathways: negative indirect influence between lipids and proteins (-8.836,  $p < 0.001$ ) and direct negative influence between carbohydrates and ash (-3.165,  $p < 0.001$ ), indicating that both immediate and cascading mechanisms contribute to carbon-allocation outcomes. These relationships capture a series of effects in which temperature alters, metabolism alters storage, and storage in turn drives lipids and carbohydrates, revealing the multi-layered nature of thermal responses.

Therefore, the SEM analysis shows that temperature does not influence each cellular character independently. Instead, it regulates a connected network that links membrane fluidity, carbon storage, and metabolic activity. By separating direct effects from indirect ones, the model reveals how temperature triggers a series of cascading responses that ultimately affect growth, fatty acids composition, proteins, lipids, carbohydrates, and ash content. This network-based view helps explain the observed results in this study, such as the shift from PUFA to MUFA, and the changes in major macromolecular. Overall, SEM provides a clearer picture of how heterotrophic microalgae adjust their physiology when temperature changes, offering a more complete understanding of

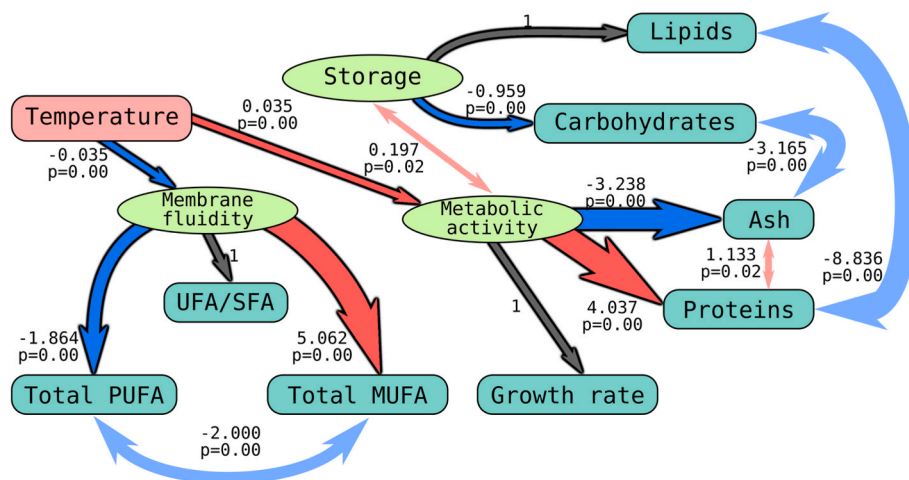


Fig. 5. Structural equation modeling (SEM) analysis of the direct and indirect pathways by temperature affects the growth and biochemical composition of *Chlorella vulgaris*. Solid red and blue arrows indicate direct positive and negative pathways; respectively, whereas light red and blue arrows represent indirect positive and negative pathways. Arrow thickness is proportional to the magnitude of the path coefficient ( $\beta$ ).

temperature-driven phenotypic plasticity in *C. vulgaris*.

#### 4. Conclusions

This study systematically revealed clear temperature-dependent change (4–35 °C) in growth, biochemical components, and fatty acid composition of *Chlorella vulgaris* under heterotrophic cultivation. Growth was optimal at 25–30 °C (1.11–1.14 day<sup>-1</sup>) and strongly inhibited at 35 °C. Although cells were able to grow at 4 °C, the lag phase was markedly prolonged, lasting up to 25 days. Biochemical composition varies with temperature, with proteins enriched at low temperatures (15 °C), lipids at higher temperatures (25 °C and 30 °C), while carbohydrates under moderate temperatures (20 °C). The adaptive response of fatty acids to temperature was primarily achieved through the interconversion of C18:2n6c and C18:3n3. These findings emphasize the thermal plasticity of *C. vulgaris* under heterotrophic conditions and provide valuable guidance for optimizing microalgal cultivation across diverse thermal environments.

#### Credit author statement

Jinjing Yin: Writing – original draft, Methodology, Investigation, Validation, Formal analysis, Conceptualization. Wendie Levasseur: Writing – review & editing, Methodology, Supervision, Formal analysis, Conceptualization. Victor Pozzobon: Writing – review & editing, Validation, Supervision, Software, Project administration, Methodology, Formal analysis, Conceptualization.

#### Declaration of competing interest

The authors declare that they have no known competing financial interests or personal relationships that could have appeared to influence the work reported in this paper.

#### Acknowledgements

Communauté urbaine du Grand Reims, Département de la Marne, Région Grand Est and European Union (FEDER Grand Est 2021–2027) are acknowledged for their financial support to the Chair of Biotechnology of CentraleSupélec and the Centre Européen de Biotechnologie et de Bioéconomie (CEBB). China Scholarship Council ([2024]52) is acknowledged for their financial support to Jinjing Yin PhD scholarship in France.

#### Appendix A. Supplementary data

Supplementary data to this article can be found online at <https://doi.org/10.1016/j.plaphy.2026.111431>.

#### Data availability

Data will be made available on request.

#### References

- Andersen, R.A., 2005. *Algal Culturing Techniques*. Academic Press.
- Barros, A., Pereira, H., Campos, J., Marques, A., Varela, J., Silva, J., 2019. Heterotrophy as a tool to overcome the long and costly autotrophic scale-up process for large scale production of microalgae. *Sci. Rep.* 9, 13935. <https://doi.org/10.1038/s41598-019-50206-z>.
- Barten, R., Djojan, Y., Evers, W., Wijffels, R., Barbosa, M., 2021. Towards industrial production of microalgae without temperature control: the effect of diel temperature fluctuations on microalgal physiology. *J. Biotechnol.* 336, 56–63. <https://doi.org/10.1016/j.jbiotec.2021.06.017>.
- Barten, R., Kleisman, M., D'Ermo, G., Nijveen, H., Wijffels, R.H., Barbosa, M.J., 2022. Short-term physiologic response of the green microalga *Picochlorum* sp. (BPE23) to supra-optimal temperature. *Sci. Rep.* 12, 3290. <https://doi.org/10.1038/s41598-022-06954-6>.
- Béchet, Q., Shilton, A., Fringer, O.B., Muñoz, R., Guieysse, B., 2010. Mechanistic modeling of broth temperature in outdoor photobioreactors. *Environ. Sci. Technol.* 44, 2197–2203. <https://doi.org/10.1021/es903214u>.
- Bligh, E.G., Dyer, W.J., 1959. A Rapid Method of Total Lipid Extraction and Purification. *Can. J. Biochem. Physiol.* 37, 911–917. <https://doi.org/10.1139/cjcp-37-6-911>.
- Chen, G., Qu, S., Wang, Q., Bian, F., Peng, Z., Zhang, Y., Ge, H., Yu, J., Xuan, N., Bi, Y., He, Q., 2014. Transgenic expression of delta-6 and delta-15 fatty acid desaturases enhances omega-3 polyunsaturated fatty acid accumulation in *Synechocystis* sp. PCC6803. *Biotechnol. Biofuels* 7, 32. <https://doi.org/10.1186/1754-6834-7-32>.
- Chen, G.-Q., Jiang, Y., Chen, F., 2008. Variation of lipid class composition in *Nitzschia laevis* as a response to growth temperature change. *Food Chem.* 109, 88–94. <https://doi.org/10.1016/j.foodchem.2007.12.022>.
- Chokshi, K., Pancha, I., Trivedi, K., George, B., Maurya, R., Ghosh, A., Mishra, S., 2015. Biofuel potential of the newly isolated microalgae *Acutodesmus dimorphus* under temperature induced oxidative stress conditions. *Bioresour. Technol.* 180, 162–171. <https://doi.org/10.1016/j.biortech.2014.12.102>.
- Converti, A., Casazza, A.A., Ortiz, E.Y., Perego, P., Del Borghi, M., 2009. Effect of temperature and nitrogen concentration on the growth and lipid content of *Nannochloropsis oculata* and *Chlorella vulgaris* for biodiesel production. *Chem. Eng. Process. Process Intensif.* 48, 1146–1151. <https://doi.org/10.1016/j.cep.2009.03.006>.
- da Silva Ferreira, V., Sant'Anna, C., 2017. The effect of physicochemical conditions and nutrient sources on maximizing the growth and lipid productivity of green microalgae. *Phycol. Res.* 65, 3–13. <https://doi.org/10.1111/pre.12160>.
- Ferrer-Ledo, N., Stegmüller, L., Janssen, M., Wijffels, R.H., Barbosa, M.J., 2023. Growth and fatty acid distribution over lipid classes in *Nannochloropsis oceanica* acclimated to different temperatures. *Front. Plant Sci.* 14, 1078998. <https://doi.org/10.3389/fpls.2023.1078998>.
- Gao, B., Hong, J., Chen, J., Zhang, H., Hu, R., Zhang, C., 2023. The growth, lipid accumulation and adaptation mechanism in response to variation of temperature and nitrogen supply in psychrotrophic filamentous microalga *Xanthonema hormidioides* (Xanthophyceae). *Biotechnol. Biofuels Bioprod.* 16, 12. <https://doi.org/10.1186/s13068-022-02249-0>.
- González-Camejo, J., Aparicio, S., Ruano, M.V., Borrás, L., Barat, R., Ferrer, J., 2019. Effect of ambient temperature variations on an Indigenous microalgae-nitrifying bacteria culture dominated by *Chlorella*. *Bioresour. Technol.* 290, 121788. <https://doi.org/10.1016/j.biortech.2019.121788>.
- Guiry, M.D., Guiry, G.M., 2025. ALGAE [WWW Document]. URL. <https://www.algaebase.org/>. accessed 6.25.25.
- Han, F., Wang, W., Li, Y., Shen, G., Wan, M., Wang, J., 2013. Changes of biomass, lipid content and fatty acids composition under a light–dark cyclic culture of *Chlorella pyrenoidosa* in response to different temperature. *Bioresour. Technol.* 132, 182–189. <https://doi.org/10.1016/j.biortech.2012.12.175>.
- Ievina, B., Romagnoli, F., 2024. Microalga *Chlorella vulgaris* 211/11j as a promising strain for low temperature climate. *J. Appl. Phycol.* 36, 1117–1124. <https://doi.org/10.1007/s10811-024-03192-3>.
- International Organization for Standardization, 2002. *Animal Feeding Stuffs — Determination of Crude Ash* (No. ISO 5984:2022). International Organization for Standardization.
- Jabeen, S., Gao, X., Altarawneh, M., Hayashi, J., Zhang, M., Długogorski, B.Z., 2020. Analytical procedure for proximate analysis of algal biomass: case study for *Spirulina platensis* and *Chlorella vulgaris*. *Energy Fuels* 34, 474–482. <https://doi.org/10.1021/acs.energyfuels.9b03156>.
- Josephine, A., Kumar, T.S., Surendran, B., Rajakumar, S., Kirubakaran, R., Dharani, G., 2022. Evaluating the effect of various environmental factors on the growth of the marine microalgae, *Chlorella vulgaris*. *Front. Mar. Sci.* 9. <https://doi.org/10.3389/fmars.2022.954622>.
- Kania, K., Drożak, A., Borkowski, A., Dziatak, P., Majcher, K., Sawicka, P.D., Zienkiewicz, M., 2023. Mechanisms of temperature acclimatization in the psychrotolerant green alga *Coccomyxa subellipsoidea* C-169 (*Trebouxiphyceae*). *Physiol. Plantarum* 175. <https://doi.org/10.1111/ppl.14034>.
- Kim, D.G., Hur, S.B., 2013. Growth and fatty acid composition of three heterotrophic *Chlorella* species. *ALGAE* 28, 101–109. <https://doi.org/10.4490/algae.2013.28.1.101>.
- Lepère, C., Masquelier, S., Mangot, J.-F., Debroas, D., Domaizon, I., 2010. Vertical structure of small eukaryotes in three lakes that differ by their trophic status: a quantitative approach. *ISME J.* 4, 1509–1519. <https://doi.org/10.1038/ismej.2010.83>.
- Levasseur, W., Perré, P., Pozzobon, V., 2020. A review of high value-added molecules production by microalgae in light of the classification. *Biotechnol. Adv.* 41, 107545. <https://doi.org/10.1016/j.biotechadv.2020.107545>.
- Liang, Y., Sarkany, N., Cui, Y., 2009. Biomass and lipid productivities of *Chlorella vulgaris* under autotrophic, heterotrophic and mixotrophic growth conditions. *Biotechnol. Lett.* 31, 1043–1049. <https://doi.org/10.1007/s10529-009-9975-7>.
- Lichtenthaler, H.K., Buschmann, C., 2001. Chlorophylls and carotenoids: measurement and characterization by UV-VIS spectroscopy. *Current Protocols in Food Analytical Chemistry* 1. <https://doi.org/10.1002/0471142913.faf0403s01>.
- Logan, J.A., Wollkind, D.J., Hoyt, S.C., Tanigoshi, L.K., 1976. An analytic model for description of temperature dependent rate phenomena in Arthropods1. *Environ. Entomol.* 5, 1133–1140. <https://doi.org/10.1093/ee/5.6.1133>.
- Lourenço, S.O., Barbarino, E., Lavin, P.L., Lanfer Marquez, U.M., Aídar, E., 2004. Distribution of intracellular nitrogen in marine microalgae: calculation of new nitrogen-to-protein conversion factors. *Eur. J. Phycol.* 39, 17–32. <https://doi.org/10.1080/0967026032000157156>.
- Lu, X., Zhao, W., Wang, J., He, Y., Yang, S., Sun, H., 2024. A comprehensive review on the heterotrophic production of bioactive compounds by microalgae. *World J. Microbiol. Biotechnol.* 40, 210. <https://doi.org/10.1007/s11274-024-03892-5>.

- Metsoviti, M.N., Papapolymerou, G., Karapanagiotidis, I.T., Katsoulas, N., 2019. Comparison of growth rate and nutrient content of five microalgae species cultivated in greenhouses. *Plants* 8, 279. <https://doi.org/10.3390/plants8080279>.
- Nakamura, Y., Miyachi, S., 1982. Change in starch photosynthesized at different temperatures in *Chlorella*. *Plant Sci. Lett.* 27, 1–6. [https://doi.org/10.1016/0304-4211\(82\)90065-7](https://doi.org/10.1016/0304-4211(82)90065-7).
- Nalley, J.O., O'Donnell, D.R., Litchman, E., 2018. Temperature effects on growth rates and fatty acid content in freshwater algae and Cyanobacteria. *Algal Res.* 35, 500–507. <https://doi.org/10.1016/j.algal.2018.09.018>.
- Peter, K.H., Sommer, U., 2013. Phytoplankton cell size reduction in response to warming mediated by nutrient limitation. *PLoS One* 8, e71528. <https://doi.org/10.1371/journal.pone.0071528>.
- Porra, R.J., 1990. A simple method for extracting chlorophylls from the recalcitrant alga, *Nannochloris atomus*, without formation of spectroscopically-different magnesium-rhodochlorin derivatives. *Biochim. Biophys. Acta Bioenerg.* 1019, 137–141. [https://doi.org/10.1016/0005-2728\(90\)90135-Q](https://doi.org/10.1016/0005-2728(90)90135-Q).
- Ras, M., Steyer, J.-P., Bernard, O., 2013. Temperature effect on microalgae: a crucial factor for outdoor production. *Rev. Environ. Sci. Biotechnol.* 12, 153–164. <https://doi.org/10.1007/s11157-013-9310-6>.
- Renaud, S.M., Thinh, L.-V., Lambrinidis, G., Parry, D.L., 2002. Effect of temperature on growth, chemical composition and fatty acid composition of tropical Australian microalgae grown in batch cultures. *Aquaculture* 211, 195–214. [https://doi.org/10.1016/S0044-8486\(01\)00875-4](https://doi.org/10.1016/S0044-8486(01)00875-4).
- Riccardo, Trentin, Moschin, E., Custódio, L., Moro, I., 2024. Temperature effects on growth, metabolome, lipidic profile and photosynthetic pigment content of *Microglona Antarctica* (chlorophyceae): a comprehensive analysis. *Algal Res.* 79, 103461. <https://doi.org/10.1016/j.algal.2024.103461>.
- Ru, I.T.K., Sung, Y.Y., Jusoh, M., Wahid, M.E.A., Nagappan, T., 2020. *Chlorella vulgaris*: a perspective on its potential for combining high biomass with high value bioproducts. *Applied Phycology* 1, 2–11. <https://doi.org/10.1080/26388081.2020.1715256>.
- Safi, C., Zebib, B., Merah, O., Pontalier, P.-Y., Vaca-Garcia, C., 2014. Morphology, composition, production, processing and applications of *Chlorella vulgaris*: a review. *Renew. Sustain. Energy Rev.* 35, 265–278. <https://doi.org/10.1016/j.rser.2014.04.007>.
- Sajadian, S., Morowvat, M., Ghasemi, Y., 2018. Investigation of autotrophic, heterotrophic, and mixotrophic modes of cultivation on lipid and biomass production in *Chlorella vulgaris*. *Natl. J. Physiol. Pharm. Pharmacol.* 8, 1. <https://doi.org/10.5455/njppp.2018.8.0935625122017>.
- Sakamoto, T., Murata, N., 2002. Regulation of the desaturation of fatty acids and its role in tolerance to cold and salt stress. *Curr. Opin. Microbiol.* 5, 206–210. [https://doi.org/10.1016/S1369-5274\(02\)00306-5](https://doi.org/10.1016/S1369-5274(02)00306-5).
- Serra-Maia, R., Bernard, O., Gonçalves, A., Bensalem, S., Lopes, F., 2016. Influence of temperature on *Chlorella vulgaris* growth and mortality rates in a photobioreactor. *Algal Res.* 18, 352–359. <https://doi.org/10.1016/j.algal.2016.06.016>.
- Shi, X., Wu, Z., Chen, F., 2006. Kinetic modeling of lutein production by heterotrophic *Chlorella* at various pH and temperatures. *Mol. Nutr. Food Res.* 50, 763–768. <https://doi.org/10.1002/mnfr.200600037>.
- Shin, H., Hong, S.-J., Yoo, C., Han, M.-A., Lee, H., Choi, H.-K., Cho, S., Lee, C.-G., Cho, B.-K., 2016. Genome-wide transcriptome analysis revealed organelle specific responses to temperature variations in algae. *Sci. Rep.* 6, 37770. <https://doi.org/10.1038/srep37770>.
- Sonmez, C., Elcin, E., Akin, D., Oktem, H.A., Yucel, M., 2016. Evaluation of novel thermo-resistant *Micractinium* and *Scenedesmus* sp. for efficient biomass and lipid production under different temperature and nutrient regimes. *Bioresour. Technol.* 211, 422–428. <https://doi.org/10.1016/j.biortech.2016.03.125>.
- Thompson, G.A., 1996. Lipids and membrane function in green algae. *Biochim. Biophys. Acta Lipids Lipid. Metabol.* 1302, 17–45. [https://doi.org/10.1016/0005-2760\(96\)00045-8](https://doi.org/10.1016/0005-2760(96)00045-8).
- Tomlinson, S., Phillips, R.D., 2015. Differences in metabolic rate and evaporative water loss associated with sexual dimorphism in thynnine wasps. *J. Insect Physiol.* 78, 62–68. <https://doi.org/10.1016/j.jinsphys.2015.04.011>.
- Van Wycken, S., Ramirez, K., Laurens, L.M.L., 2016. Determination of total lipids as Fatty Acid Methyl Esters (FAME) by in situ transesterification: Laboratory analytical procedure (LAP). <https://doi.org/10.2172/1118085>.
- Wang, K., Wang, Z., Ding, Y., Yu, Y., Wang, Y., Geng, Y., Li, Y., Wen, X., 2023. Optimization of heterotrophic culture conditions for the algae *Graesiella emersonii* WBG-1 to produce proteins. *Plants* 12, 2255. <https://doi.org/10.3390/plants12122255>.
- Xie, W., Li, X., Xu, H., Chen, F., Cheng, K.-W., Liu, H., Liu, B., 2023. Optimization of heterotrophic culture conditions for the microalgae *Euglena gracilis* to produce proteins. *Mar. Drugs* 21, 519. <https://doi.org/10.3390/md21100519>.
- Xin, L., Hong-ying, H., Yu-ping, Z., 2011. Growth and lipid accumulation properties of a freshwater microalga *scenedesmus* sp. under different cultivation temperature. *Bioresour. Technol.* 102, 3098–3102. <https://doi.org/10.1016/j.biortech.2010.10.055>.
- Xing, C., Li, J., Yuan, H., Yang, J., 2022. Physiological and transcription level responses of microalgae *Auxenochlorella protothecoides* to cold and heat induced oxidative stress. *Environ. Res.* 211, 113023. <https://doi.org/10.1016/j.envres.2022.113023>.
- Xing, G., Yuan, H., Yang, J., Li, J., Gao, Q., Li, W., Wang, E., 2018. Integrated analyses of transcriptome, proteome and fatty acid profilings of the oleaginous microalga *Auxenochlorella protothecoides* UTEX 2341 reveal differential reprogramming of fatty acid metabolism in response to low and high temperatures. *Algal Res.* 33, 16–27. <https://doi.org/10.1016/j.algal.2018.04.028>.
- Yu, J., Wang, C., Su, Z., Xiong, P., Liu, J., 2014. Response of microalgae growth and cell characteristics to various temperatures. *Asian J. Chem.* 26, 3366–3370. <https://doi.org/10.14233/ajchem.2014.17529>.
- Zhang, K., Sun, B., She, X., Zhao, F., Cao, Y., Ren, D., Lu, J., 2014. Lipid production and composition of fatty acids in *Chlorella vulgaris* cultured using different methods: photoautotrophic, heterotrophic, and pure and mixed conditions. *Ann. Microbiol.* 64, 1239–1246. <https://doi.org/10.1007/s13213-013-0766-y>.
- Zhang, Q., Zhan, J., Hong, Y., 2016. The effects of temperature on the growth, lipid accumulation and nutrient removal characteristics of *Chlorella* sp. HQ. *Desalination Water Treat.* 57 (iv). <https://doi.org/10.1080/19443994.2015.1051790>.
- Zhao, Y., Sun, Y., Zhu, Z., Li, Y., Zhang, L., Li, J., Agathos, S.N., Zhou, C., Han, J., 2024. Effects of salinity and temperature on growth performance, biochemical composition, and biosilification process of *Cyclotella cryptica*. *Algal Res.* 84, 103751. <https://doi.org/10.1016/j.algal.2024.103751>.
- Zhou, Y., Jiang, L., Weng, Y., Zong, H., Li, Z., Xu, J., Li, F., 2025. Growth characteristics and nutritional quality of two typical microalgae: interactive effects of temperature, light, and nitrate. *Algal Res.* 104004. <https://doi.org/10.1016/j.algal.2025.104004>.
- Zhu, C.J., Lee, Y.K., Chao, T.M., 1997. Effects of temperature and growth phase on lipid and biochemical composition of *Isochrysis galbana* TK1. *J. Appl. Phycol.* 9, 451–457. <https://doi.org/10.1023/A:1007973319348>.
- Zorin, B., Pal-Nath, D., Lukyanov, A., Smolskaya, S., Kulusheva, S., Didi-Cohen, S., Boussiba, S., Cohen, Z., Khozin-Goldberg, I., Solovchenko, A., 2017. Arachidonic acid is important for efficient use of light by the microalga *Lobosphaera incisa* under chilling stress. *Biochim. Biophys. Acta Mol. Cell Biol. Lipids* 1862, 853–868. <https://doi.org/10.1016/j.bbalip.2017.04.008>.